



Acidic hierarchical porous ZSM-5 assembled palladium catalyst: A green substitute to transform primary amides to nitriles

Zhongmiao Chen^a, Wei Chen^{b,*}, Lei Zhang^a, Wenqian Fu^a, Guoren Cai^a, Anmin Zheng^b, Tiandi Tang^{a,*}

^a Jiangsu Key Laboratory of Advanced Catalytic Materials and Technology, School of Petrochemical Engineering, Changzhou University, Changzhou, Jiangsu 213164, PR China

^b State Key Laboratory of Magnetic Resonance and Atomic and Molecular Physics, National Center for Magnetic Resonance in Wuhan, Wuhan Institute of Physics and Mathematics, Innovation Academy for Precision Measurement Science and Technology, Chinese Academy of Sciences, Wuhan 430071, PR China

ARTICLE INFO

Keywords:

Zeolites
Acidity
Pd catalyst
Reaction mechanism
Primary amides to nitriles

ABSTRACT

Metal catalyzed dehydration of primary amides is an attractive route for the synthesis of nitriles, but this transformation is often promoted by various environmentally hazardous additives or organic ligands in homogeneous catalysis, which limits its industrial application. The acidic mesoporous ZSM-5 assembled palladium (Pd/ZSM-5-H) was found to be able to systemically convert primary amides to nitriles in the absence of any additives with excellent applicability. The highly dispersive Pd(II) species grafted on ZSM-5-H via the strong binding interaction between AlO_4 tetrahedron and Pd species (Pd/ZSM-5-H) drive the significantly higher reaction activity (100%) than Pd/Silicalite-1-H (30%) and $\text{Pd}(\text{OAc})_2$ (20%). Furthermore, the active centers of Pd/ZSM-5-H in the catalytic process were attributed to $[\text{PdOH}]^+$ by the acidity characterization and theoretical calculations, and the primary amides to nitriles catalyzed by $[\text{PdOH}]^+$ in Pd/ZSM-5-H is thermodynamically and kinetically favorable with $-\text{OH}$ group in $[\text{PdOH}]^+$ as an agent of proton transfer.

1. Introduction

Developing a simple and clean reaction system with high efficiency is very important to access the industrial application and product manufacture for the synthesis of fine organic chemicals. Commonly, most organic synthesis routes and methodologies on laboratory and industry are complicated by introducing metal salt catalysts, organic ligands as well as diverse additives to obtain a high yield of the target product [1–3]. Nitriles, as the broadly part of industrial application on dyes, herbicides, agrochemicals, pharmaceuticals, biologically active agents, and natural products [4–7], was synthesized by various methods. However, the traditional Sandmeyer reaction from anilines and the Rosenmund–von Braun reaction from aryl halides have nearly prohibited their broadly applications due to highly toxic cyanide sources [8]. On the other hand, ammoxidation of n-propene to acrylonitrile and hydrocyanation of 1,3-butadiene to adiponitrile are available methods in mass-produce nitriles, but limited by the harsh reaction conditions [9].

Alternatively, direct synthesis of nitriles by dehydration of amides

may be one of the fundamental and clean synthetic routes, and dehydrating agents under simple reaction conditions is particularly attractive from the green chemistry point of view. The current dehydration methods of amides to nitriles can be divided into non-catalyzed and catalyzed methods, and the catalytic dehydrations can be basically divided into transition metal, non-transition metal, organo-catalysts in the presence of acetonitrile (CH_3CN) and silyl compounds as summarized in Fig. 1. No matter what methods were employed to dehydrate amides to nitriles, the detrimental compounds including numerous additives and vast of solvents are inevitable, especially the highly toxic Selectfluor, chlorinated organic compounds and organophosphorus reagents [10–13]. Therefore, the development of highly efficient and environmentally friendly catalysts to synthesize nitriles is very important to improve current situations. During the synthesis methods, palladium (Pd) catalysts are one types of frequently used one with high yield and selectivity to nitriles, including PdCl_2 , $\text{Pd}(\text{O}_2\text{CCF}_3)_2$, $\text{Pd}(\text{OAc})_2$, $\text{PdCl}(\text{PPh}_3)_2$ with the help of additives, like H_2O , Selectfluor, LiCl/AgOAc , $\text{Cu}(\text{OAc})_2$, etc [14–20]. Although Pd(II) homogeneous catalysts have the advantages on yield and selectivity, environmental

* Corresponding authors.

E-mail addresses: chenwei@wipm.ac.cn (W. Chen), tangtiandi@cczu.edu.cn (T. Tang).

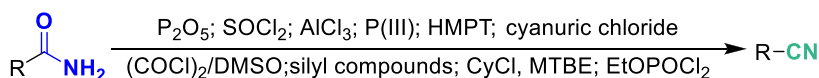
<https://doi.org/10.1016/j.apcatb.2021.120835>

Received 19 July 2021; Received in revised form 15 October 2021; Accepted 16 October 2021

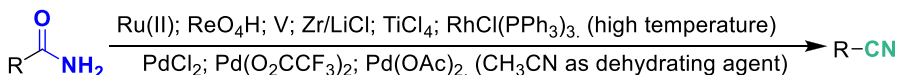
Available online 24 October 2021

0926-3373/© 2021 Elsevier B.V. All rights reserved.

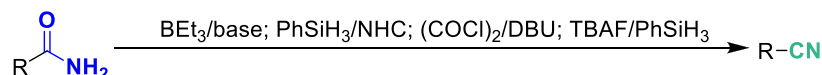
(a) Non-catalyzed dehydration of amides using chemical reagents



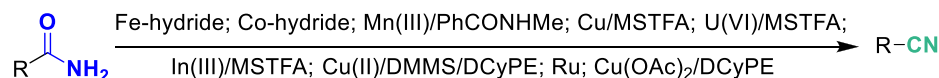
(b) Metal-catalyzed dehydration at high temperature or using acetonitrile as dehydrating agent



(c) Non-transition metal catalyzed dehydration



(d) Transition metal catalyzed silylative dehydration



(e) Heterogeneous catalysts dehydration

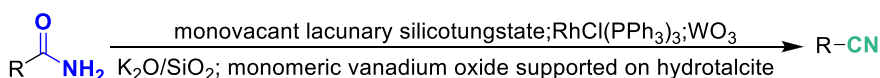


Fig. 1. Dehydration of amides to nitriles by different catalysts.

requirements promote the development of new catalysts without any additives.

Heterogeneous catalysts have realized many examples translating enzymatic and homogeneous catalysis to heterogeneous catalysis [21–23]. Moreover, the reaction mixtures and catalysts can be straightforwardly separated without large costing, and expensive catalysts (like Pd catalysts in homogeneous catalysis) can be easily and effectively recycled. Furthermore, the active sites in heterogeneous catalysts usually can produce the target products with high efficiency and selectivity by unique local chemical environment (such as coordination, pore confinement, etc.), and that may avoid some hazardous additives. Although RhCl(PPh₃)₃ [24], silica supported potassium oxide [25], monomeric vanadium oxide supported on hydrotalcite [26] and etc [27,28] have acted as heterogeneous catalysts to convert amides to nitriles, the dehydration over these heterogeneous catalysts mainly occurred at the surface with low efficiency. Some heterogeneous catalysts with micropores or mesopores, like zeolite, metal-organic frameworks, and covalent-organic frameworks, have not been used to further improve catalytic performance. In this context, Pd(II) active sites in homogeneous catalysis may be ready to transplant into porous heterogeneous catalyst. As a kind of typical heterogeneous catalysts, zeolites can not only use Lewis and Brønsted acidic sites in acidic catalysis, but also can act as the support to graft metal ions or metal-oxide for realizing some specific applications. Pd/zeolite catalysts have been successfully used to methane oxidation [29–32], biomass hydrogenation [33,34], and thiophenes vinylation [35] by different synthesis methods, loading ways, zeolite types, etc. Herein, two zeolites with the same MFI topology, ZSM-5-H and Silicalite-1-H, were used to graft single Pd(II) active site for evaluating the influence of the Lewis and Brønsted acidic sites to support Pd(II) and the catalytic activity to selectively transform amides to nitriles. Moreover, SiO₂ was also considered as Pd(II) support material to compare the effect of porous structure to the catalytic activity.

2. Catalyst synthesis and characterization

2.1. Support materials synthesis

Hierarchical porous ZSM-5 zeolite (ZSM-5-H) was synthesized in the presence of tetraethylammonium hydroxide (TEAOH) from an aluminosilicate gel with a molar composition of Al₂O₃/84SiO₂/23Na₂O/2.9TEAOH/2550H₂O. The cationic copolymer containing quaternary ammonium groups (CCQA) was used as mesoporous template and its detailed synthesis procedure is presented in Supporting Information. The hydro-thermal synthesis was performed in a 300 mL Parr autoclave equipped with 4836 controller. In a typical run, 60 mL of industrial water glass (26.0% SiO₂, 7.3% Na₂O, 66.7% H₂O), 37.7 mL H₂O and 9.4 mL TEAOH (25 wt%) was mixed for stirring 1 h. Then, 25 mL CCQA slowly add into the mixture under vigorous stirring. After stirring for 2 h, an acidic Al₂(SO₄)₃ aqueous solution (dissolving 2.7 g Al₂(SO₄)₃·18H₂O in 18.8 mL dilute sulfuric acid) was added. The mixture was stirred for 2 h to yield an aluminosilicate gel and further heated to 170 °C for crystallization 2 days. After the reaction was finished and the reactor was cooled to room temperature, the reaction mixture was separated by filtration method. The obtained solid sample was washed by deionized water, and it was dried at 120 °C overnight and calcined in air at 550 °C for 5 h. The H-form of the ZSM-5-H zeolite was obtained by ion exchange with NH₄NO₃ solution (1 M) after drying and calcination of the exchanged sample. Microporous zeolite ZSM-5 was synthesized as the same procedure in the absent of mesoporous template.

Hierarchical porous pure silicon ZSM-5 zeolite (Silicalite-1-H) was synthesized in the presence of TEAOH from a silicate gel with a molar composition of 86.8SiO₂/19.7TEAOH/ 2000H₂O, and the *N,N*-dimethyl-*N*-octadecyl-*N*-(3-triethoxysilylpropyl) ammonium [(C₂H₅O)₃SiC₃H₆N(CH₃)₂C₁₈H₃₇]⁺ cation as a mesoscale template. In a typical run, 20 mL of tetraethoxysilane, 24 mL H₂O and 16 mL TEAOH (25 wt%) were mixed for stirring 3 h. 7 mL mesoscale template was slowly added to the mixture under vigorous stirring. After stirring at room temperature for 2 h, the obtained gel was transferred into a Teflon lined stainless steel autoclave for static crystallization at 180 °C for 3 days. After filtration

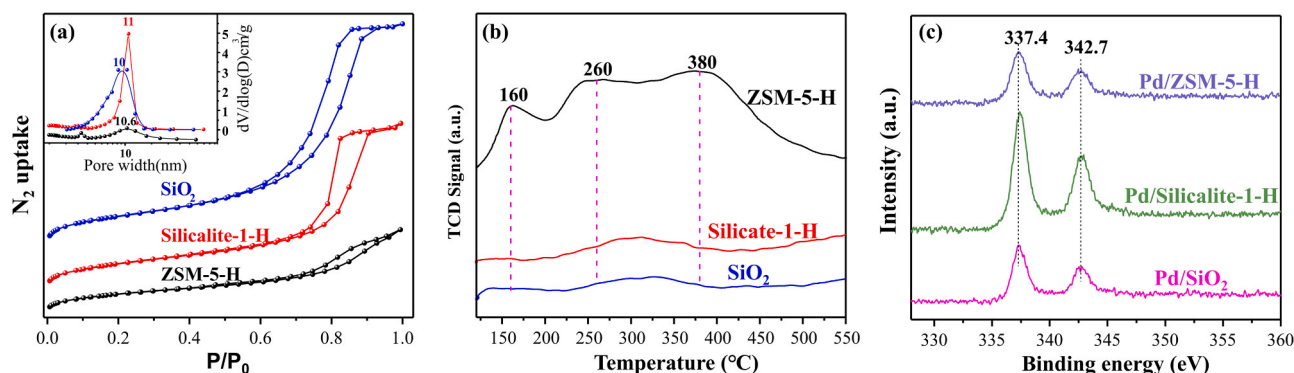


Fig. 2. (a) N₂-adsorption isotherms and mesoporous size distribution of the samples, (b) NH₃-TPD curves of the samples, (c) XPS spectra of Pd(II) of the supported Pd catalysts.

Table 1

Textural parameters of the series of supports.

Samples	S_{BET} (m ² g ⁻¹) ^a	S_{ext} (m ² g ⁻¹) ^b	Pore width (nm)	V_{micro} (cm ³ g ⁻¹) ^c	V_{meso} (cm ³ g ⁻¹) ^d	Si/Al	Benzamide uptake	
							Uptake (mg/g _{cat})	mmol/m ^{2c}
ZSM-5-H	458	217	10.6	0.10	0.37	40	21.5	8.2×10^{-4}
Silicalite-1-H	462	304	11.0	0.07	0.74	–	6.5	1.8×10^{-4}
SiO ₂	362	330	10.0	0.01	0.94	–	6.3	1.6×10^{-4}

^a BET surface area.

^b External surface area.

^c Microporous volume.

^d Mesoporous volume.

^e The moles of benzamide adsorbed are based on the unit external surface area of the support.

and washing, the sample was dried at 120 °C overnight and calcined in air at 550 °C for 5 h.

2.2. Characterization of support materials

The texture parameter of the support samples was analyzed by nitrogen adsorption experiment on a Micromeritics TriStar II 3020 at liquid nitrogen temperature (−196 °C). Brunauer-Emmett-Teller (BET) surface area was calculated by using adsorption data. The mesopore size distribution was obtained using the desorption data according to the Barrett-Joyner-Halenda (BJH) model. Transmission electron microscopy (TEM) image of the catalyst was obtained on a JEM-2100F microscope with a limited line resolution capacity of 1.4 Å at 200 kV. Before characterization by TEM technique, the sample was cut into thin slices and dropped onto a carbon-coated Cu grid.

Acidity of the support materials was measured by ammonia temperature-programmed desorption (NH₃-TPD) on a Micromeritics ASAP 2920 instrument. Typically, 200 mg of the sample was placed in a quartz tube and pretreated with a helium stream at 450 °C for 2 h. After the sample was cooled down to 120 °C, an NH₃-He gas mixture (10 vol% NH₃) was flowed over the sample for 30 min. After removing the physically adsorbed NH₃ by flowing helium for 2 h at 120 °C, the sample was heated from 120 °C to 600 °C at a rate of 10 °C min⁻¹. The acidic characteristic of the support was further investigated by infrared spectroscopy of chemisorbed pyridine on a Bruker TENSOR 27 spectrometer. The powder sample (10 mg) was pressed into a self-supporting wafer. Heat treatment of the wafer was performed in a cell at 2 h in dynamic vacuum. Subsequently, the sample was cooled down to room temperature and adsorbed by pyridine. Finally, they were outgassed overnight at 200 °C before the IR measurement. The sample of benzamide-chemisorbed on zeolite was also investigated on a same infrared spectrophotometer equipped with a reactor cell. Before measurement, the sample was evacuated to 10⁻² Pa at 80 °C for 10 h. The spectrum was obtained in absorbance mode and was shown after subtraction of a

background spectrum obtained on the corresponding pure zeolite sample at 50 °C under vacuum.

The pore structure and acidity of ZSM-5-H, Silicalite-1-H and SiO₂ were characterized by N₂ −196 °C adsorption isotherm and NH₃-TPD as displayed in Fig. 2a,b. N₂ isotherms of ZSM-5-H, Silicalite-1-H and SiO₂ exhibit a step at 0.6–0.9 (P/P₀), which are typically assigned to the presence of mesoporous structure. Correspondingly, the pore-size distributions of SiO₂, Silicalite-1-H and ZSM-5-H are centered at 10–11 nm, respectively. The high external surface area and mesoporous structure in supporting material are very important, which is necessary for providing the coordination space of reactant molecule with catalyst active sites. As summarized in Table 1, the BET surface area (S_{BET}) of ZSM-5-H (458 m²/g) and Silicalite-1-H (462 m²/g) are much higher than those of SiO₂ (362 m²/g), and the larger microporous pore volume of ZSM-5-H (0.10 cm³/g) indicate more possibility to graft Pd(II) with the higher confinement effect to reactants than these of 0.07 and 0.01 cm³/g for Silicalite-1-H and SiO₂. Furthermore, the NH₃-TPD curves shows that ZSM-5-H sample has abundant weak, middle, and strong acidic sites, while the acidity of Silicalite-1-H and SiO₂ samples is negligible (Fig. 2b). The sample with the abundant porosity and highest acidity display the better performance on catalytic reaction because of the rapid diffusion of the reactant or products in hierarchical ZSM-5 [36]. All these characterizations of supporting materials indicate that ZSM-5-H may be ready to support Pd(II) by more abundant Brønsted and Lewis acidic sites than Silicalite-1-H and SiO₂.

2.3. Catalyst preparation

The typical procedures of the catalyst preparation are as follows. 50 mg of Pd(NO₃)₂·2H₂O was dissolved in 100 mL of dilute nitric acid solution (pH 2–3), then 1 g support was added under stirring. The slurry was stirred at room temperature for 3 days. After filtration and washing, the obtained solid sample was dried at 60 °C overnight. The obtained catalysts with different supports are designated as Pd/ZSM-5-H, Pd/

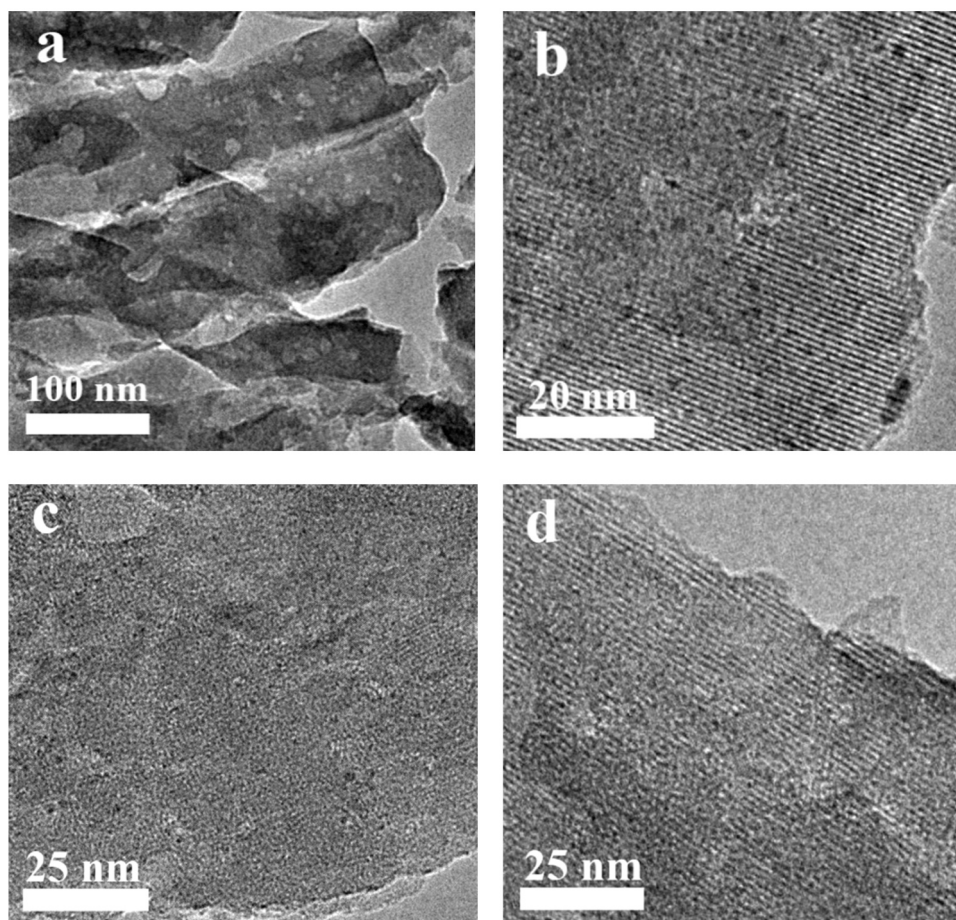


Fig. 3. Low (a) and high (b, c and d)-resolution TEM image of Pd/ZSM-5-H sample.

Silicalite-1-H and Pd/SiO₂, and the metal loadings on three catalysts are 1.7, 1.9 and 1.7 wt%, respectively, which was analyzed by inductively coupled plasma optical emission spectroscopy with a Perkin-Elmer 3300DV emission spectrometer.

After introduced Pd species, the oxidation state of Pd in Pd/ZSM-5-H, Pd/Silicalite-1-H and Pd/SiO₂ catalysts was characterized by X-ray photoelectron spectroscopic (XPS) experiments on an ESCALAB MK II system, and the binding energies at 337.4 eV(3d_{5/2}) and 342.7 eV(3d_{3/2}) in the XPS spectra of Fig. 2c were the character of Pd(II) [37]. Pd in Pd/ZSM-5-H, Pd/Silicalite-1-H and Pd/SiO₂ catalysts has the same oxidation state of Pd(II) as the homogenous catalysts of PdCl₂, Pd(OAc)₂,

and Pd(O₂CCF₃)₂ [14–20], which may lead to the high catalytic activity of Pd/ZSM-5-H, Pd/Silicalite-1-H and Pd/SiO₂ catalysts.

Moreover, the low-resolution TEM image shows that the mesopore cavities (light dots) are presented in ZSM-5-H crystals (Fig. 3a and Fig. S1). The high-resolution TEM image shows that the Pd species in the form of clusters are highly scattered in disordered mesopores and confined in the ordered micropores (Fig. 3b and Fig. S2), which is attributed to the fact that the ZSM-5-H crystals contain both hierarchical mesopores and ordered micropores (0.54 nm). Some metal clusters with size of 1–2 nm are dispersed in the micro-mesoporous channels (Fig. 3b and Fig. S2). In addition, partial of metal clusters with size less than

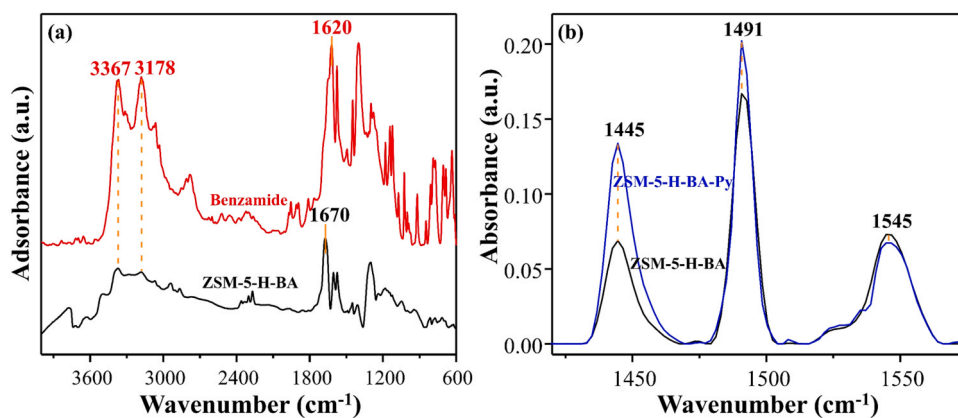


Fig. 4. (a) IR spectra of the pure benzamide and the benzamide adsorbed on ZSM-5-H (ZSM-5-H-BA) sample. (b) IR spectra of the ZSM-5-H-BA and ZSM-5-H-BA-Py samples.

1 nm are inconspicuously scattered on the surface of the catalyst, which can be observed in different selected zones (Fig. 3c, d and Fig. S3). Possibly, these clusters are embedded in the micropore mouths that open on the mesoporous surface of the ZSM-5-H support. And the X-ray energy dispersive spectroscopy (EDS) mapping of the selected zone confirms the presence of Pd species (Fig. S4).

Furthermore, relative to Pd/Silicalite-1-H and Pd/SiO₂, the abundant acidic sites on Pd/ZSM-5-H catalyst can favor the adsorption of the amides (like benzamide), which greatly improve the reaction activity. This suggestion was strongly supported by the benzamide adsorption experiments and the IR analysis of the benzamide-adsorbed ZSM-5-H sample. The adsorption capacity of ZSM-5-H (21.5 mg/g_{Cat}) is much higher than that of Silicalite-1-H and SiO₂ (6.5 and 6.3 mg/g_{Cat}, Table 1), confirming that the abundant acidic sites on the Pd/ZSM-5-H catalyst are more favorable for the adsorption of benzamide molecules. This conclusion was further demonstrated by the IR spectra of the pure benzamide and the ZSM-5-H adsorbing benzamide sample (ZSM-5-H-BA) at room temperature (Fig. 4a).

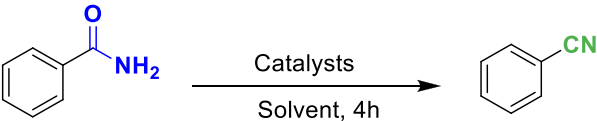
From Fig. 4a, the absorption band at 3367 and 3178 cm⁻¹ associated with the characteristic of N-H stretching vibrations, and the band at 1620 cm⁻¹ associated with the characteristic of C=O stretching vibration were observed in the IR spectrum for the pure benzamide sample. After the benzamide adsorbed on the ZSM-5-H, the characteristic of C=O band at 1620 cm⁻¹ was shifted to 1670 cm⁻¹ for the ZSM-5-H-BA sample. This result indicates that the acylamino in benzamide molecule can interact with acidic sites on ZSM-5-H. To further confirm this suggestion, another pyridine adsorption experiment was performed using ZSM-5-H-BA sample. The pyridine adsorbed on ZSM-5-H-BA sample was denoted as ZSM-5-H-BA-Py. The ZSM-5-H-BA-Py was employed to obtain an IR spectrum and the result is presented in Fig. 4b. For comparison, the IR spectrum of the ZSM-5-H-Py is given as well. Clearly, the intensity of absorption peak at 1445 cm⁻¹ associated with Lewis acid characteristic on the ZSM-5-H-BA-Py sample is significantly weakened, while the intensity of 1545 cm⁻¹ band associated with Brønsted acidity is almost no changed, as compared to ZSM-5-H-Py sample. According to above results, it can be concluded that the benzamide molecules are indeed adsorbed on ZSM-5-H through acylamino interacted with Lewis acidic sites. The benzamide molecules adsorbed on Pd/ZSM-5-H catalyst could benefit its coordination with Pd active sites (this is discussed in reaction mechanism as follow). The Lewis acid strengths of Silicalite-1-H and SiO₂ are very weak (Fig. 2b), which is not enough to promote proper interaction of the acidic site with benzamide molecule. Thus, the Pd/Silicalite-1-H and Pd/SiO₂ catalysts should present a lower activity as compared to Pd/ZSM-5-H catalyst. Moreover, the XRD patterns of ZSM-5-H and Pd/ZSM-5-H shows characteristic peaks in the range of 5–50° are related to the typical MFI structure. The additional peaks associated with Pd species were not detected, suggesting that the Pd species with small sized dispersed on zeolite or located in ion-exchanged sites in zeolite (Fig. S5). Furthermore, the similar XRD patterns of ZSM-5-H and Pd/ZSM-5-H also indicate that the hierarchical mesopores and ordered micropores of ZSM-5-H was basically unchanged after Pd species introduction. Note that the hierarchical porous Pd/ZSM-5 was proved to be the higher catalytic lifetime than the regular Pd/ZSM-5 on methane oxidation by Petrov et al., [30,31]. Therefore, the hierarchical mesopores and ordered micropores of Pd/ZSM-5-H in this work would have the benefits on catalytic lifetime.

2.4. Activity test

A typical experimental procedure for the dehydration of benzamide to form benzonitrile was as follows: powdered catalyst (20 mg), benzamide (0.2 mmol), and acetonitrile (CH₃CN, 1.5 mL) were placed in a sealed tube (10 mL) under air atmosphere. The sealed tube was put in an oil bath with temperature of 100 °C for 4 h. The reaction temperature and stirring rate was controlled using an IKA stirrer (model of RTC BS025). When the reaction was finished, the sealed tube was removed

Table 2

Synthesis of benzonitrile over a series of catalysts in different solvents^a.



Entry	Catalysts	Solvent	Temp. (°C)	TON ^b	Conv. (%) ^c	Select. (%) ^c
1	ZSM-5-H	CH ₃ CN	100	—	—	—
2 ^c	Pd(OAc) ₂	CH ₃ CN	100	2.0	20	100
3	Pd/SiO ₂	CH ₃ CN	100	11.3	18	100
4	Pd/Silicalite-1-H	CH ₃ CN	100	15.9	30	100
5	Pd/ZSM-5-H	CH₃CN	100	62.5	100	100
6	Pd/ZSM-5-H	CH ₃ CN	90	56.3	90	100
7	Pd/ZSM-5-H	CH ₃ CN	80	46.9	75	100
8	Pd/ZSM-5-H	THF	100	3.8	6	100
9	Pd/ZSM-5-H	DMF	100	—	—	—
10	Pd/ZSM-5-H	1,4-dioxane	100	—	—	—
11	Pd/ZSM-5-H	toluene	100	—	—	—
12	Pd/ZSM-5-H-C^d	CH₃CN	100	—	—	—
13	Pd/ZSM-5-H-R ^e	CH ₃ CN	100	—	—	—
14	Pd/ZSM-5 ^f	CH ₃ CN	100	—	16	100

^a Reaction conditions: Benzamide (0.2 mmol), Solvent (2 mL), catalyst (20 mg).

^b The conversion number of reactant molecules is based on the unit mole number of metals.

^c The data was obtained by GC 7890B analysis, ^c0.02 mmol Pd(OAc)₂.

^d The Pd/ZSM-5-H was calcined at 450 °C in air for 2 h.

^e The calcined Pd/ZSM-5-H was reduced at 450 °C in H₂ stream for 2 h.

^f ZSM-5 is the microporous ZSM-5 without mesopores.

from the oil bath and cooled down to room temperature. The liquid product was obtained by centrifugation from the reaction mixture and analyzed by using an Agilent 7890B GC equipped with a flame ionization detector. Additionally, the pure product was obtained by flash column chromatography on silica gel using petroleum ether (60–90 °C) and ethyl acetate as eluents.

3. Result and discussion

3.1. High activity of Pd/ZSM-5-H catalyst

The above characterizations reveal the tremendous potential of Pd/ZSM-5-H to catalyze amides to nitriles, herein, the catalytic activity of Pd/ZSM-5-H catalyst was first tested by the dehydration of benzamide to benzonitrile in different solvents, as well as a series of analogous catalysts at different reaction temperatures for comparison (Table 2). The metal-free ZSM-5-H is inactive (entry 1) without the Pd(II) active site. But when Pd species were grafted on ZSM-5-H, the convert ratio (CONV.) and selectivity (Select.) of benzamide to benzonitrile reached 100% with turn over number (TON) of 62.5, which is much higher than these of Pd/Silicalite-1-H, Pd/SiO₂ and the dissociative Pd(OAc)₂ catalysts as we expected by above characterizations (entries 2–5). Note that Pd/ZSM-5-H catalyst usually have 100% selectivity to convert benzamide to benzonitrile, (entry 5–8) but this catalyst was quite sensitive to reaction temperature and solvents. 100 °C has been proved to be the optimal reaction temperature, neither increasing or decreasing temperatures based on 100 °C would reduce the catalytic efficiency of Pd/ZSM-5-H. Notably, CH₃CN, as a solvent, has much higher effect to promote the dehydration of benzamide to benzonitrile than THF (entry 8–11), and CH₃CN was also a dehydrating agent according to the Pd(OAc)₂ and PdCl₂ homogeneous catalysis experiments [14,15]. To figure out the

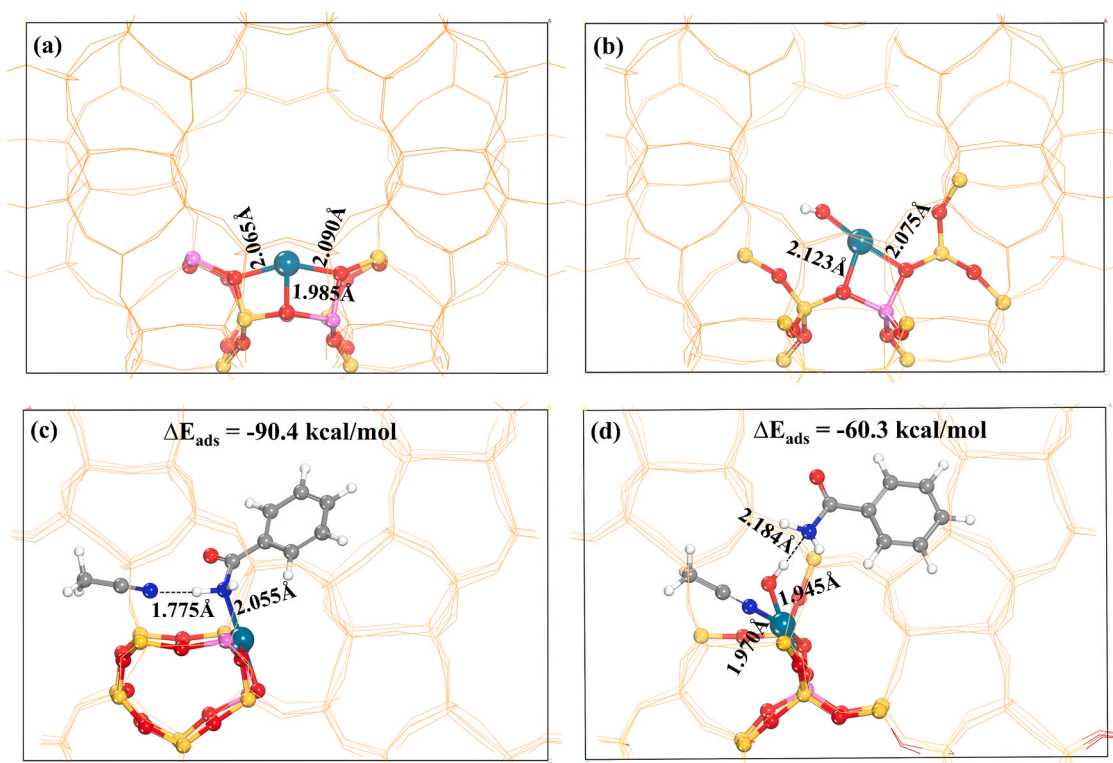


Fig. 5. The optimized structures of (a) [Pd]²⁺/ZSM-5 and (b) [Pd-OH]⁺/ZSM-5, and the optimized structures of co-adsorbed PhCONH₂ and CH₃CN on (c) [Pd]²⁺/ZSM-5 and (d) [Pd-OH]⁺/ZSM-5 by periodic PBE-D3 functional.

chemical formula of active center in Pd/ZSM-5-H, the Pd/ZSM-5-H was calcined at 450 °C in air and H₂ stream to remove the possibly extra group of Pd[II] species, the remaining single Pd[II] active sites were considered as active center to catalyze the dehydration of benzamide in Pd(OAc)₂ by Al-Huniti et al., [15] but the obtained two catalysts are both completely deactivated (entry 12–13). Therefore, some additional groups (such as -OH group) with Pd[II] (i.e., [Pd-OH]⁺) should be synergistically catalyze the conversion of benzamide to benzonitrile. Furthermore, the selectivity to benzonitrile over Pd/ZSM-5-H are always 100% during five catalytic cycles, and the conversion ratio slightly reduce from 100% in the first catalytic cycle to 95% in the fifth catalytic cycle. Pd/ZSM-5-H reveals the high recyclability in the conversion of benzamide dehydration to benzonitrile as displayed in Fig. S6.

3.2. Active center and reaction mechanism of Pd/ZSM-5 catalyst

To confirm above speculation, we further employed theoretical calculations to verify the reaction mechanism of primary amides to nitriles over [Pd]²⁺ or [Pd-OH]⁺ grafted on ZSM-5 for comparison, i.e., [Pd]²⁺/ZSM-5 and [Pd-OH]⁺/ZSM-5. To construct [Pd]²⁺/ZSM-5, two negative charges by two substitutive Al atoms in T12 and T3 sites were introduced to neutralize [Pd]²⁺, but only one substitutive Al atom in T12 site was used to graft [Pd-OH]⁺ as displayed in Fig. 5a and b. As the key step, the adsorption of reactants on active sites were critical for the overall reaction, and the co-adsorptions of CH₃CN and PhCONH₂ on [Pd]²⁺/ZSM-5 and [Pd-OH]⁺/ZSM-5 were illustrated in Fig. 5c and d. Notably, reactants show completely different adsorption behaviors on [Pd]²⁺/ZSM-5 and [Pd-OH]⁺/ZSM-5. In [Pd]²⁺/ZSM-5, -NH₂ group in

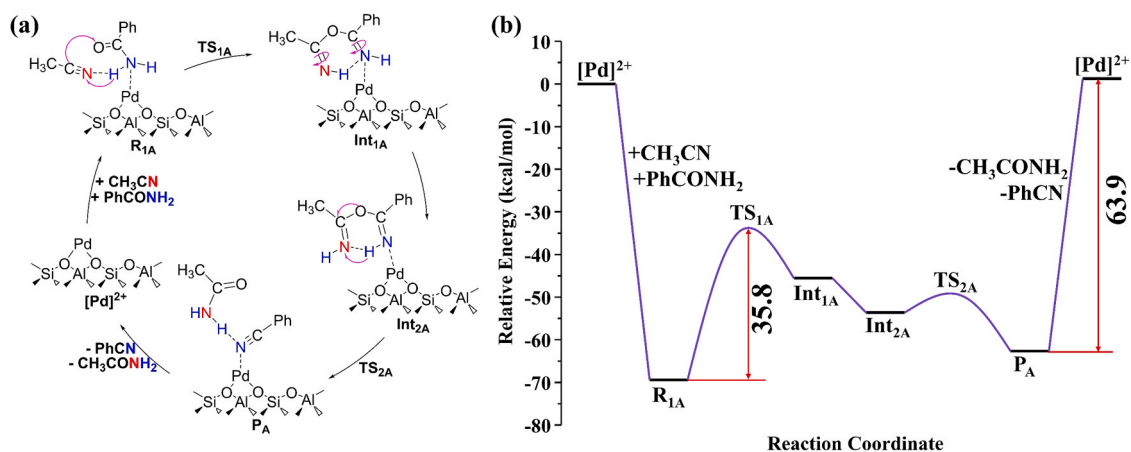


Fig. 6. (a) Reaction scheme and (b) potential energy surface of PhCONH₂ + CH₃CN to PhCN + CH₃CONH₂ over [Pd]²⁺/ZSM-5 at B3LYP-D3BJ/6-311G(d, p)/LanL2DZ level of theory. All energies have been corrected by zero-point energy.

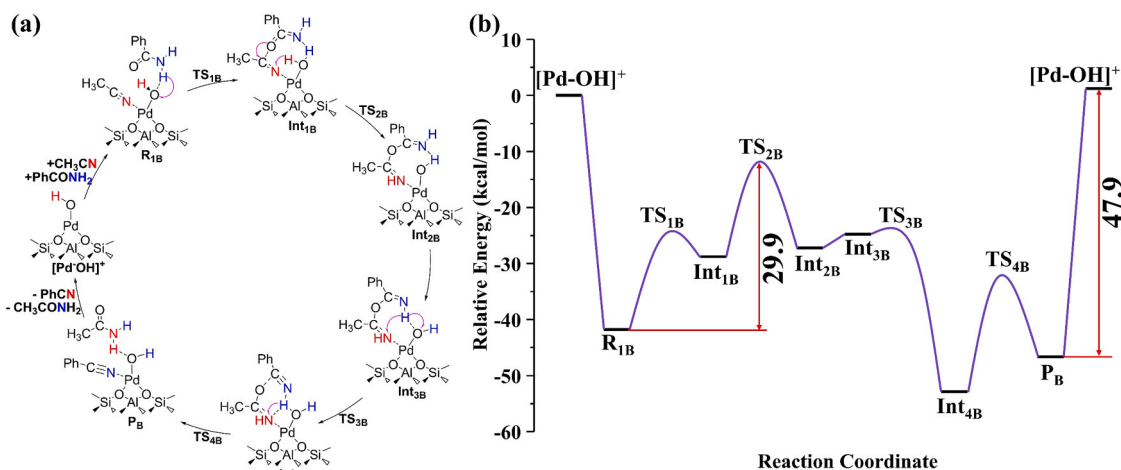


Fig. 7. (a) Reaction scheme and (b) potential energy surface of PhCONH₂ + CH₃CN to PhCN + CH₃CONH₂ over [PdOH]⁺/ZSM-5 at B3LYP-D3BJ/6-311G(d, p)/LanL2DZ level of theory.

PhCONH₂ adsorbs on the Pd atom by coordinate interaction, and CH₃CN was adsorbed on the hydrogen atoms of -NH₂ group in adsorbed PhCONH₂ by hydrogen bond interaction. But in [Pd-OH]⁺/ZSM-5, PhCONH₂ interacts with -OH group by hydrogen bond interaction, and CH₃CN was adsorbed on the Pd atom by coordinate interaction. This different adsorption behaviors on [Pd]²⁺/ZSM-5 and [Pd-OH]⁺/ZSM-5 lead to the significant difference on adsorption energies, which may further indicate the different reaction pathways on the conversion of benzamide to benzonitrile.

Due to the proximity of -NH₂ and -CN groups in the geometry of PhCONH₂ and CH₃CN co-adsorbed on [Pd]²⁺/ZSM-5, the hydrogen atoms of -NH₂ group can be directly accepted by -CN group with the gradually approaching distance between oxygen (-CONH₂ group) and carbon (-CN group) by overcoming two energy barriers as displayed in Fig. 6. The first proton transfer from -NH₂ group to -CN group is the rate-determining step with a barrier of 35.8 kcal/mol, and the strong adsorption of CH₃CONH₂ and PhCN on [Pd]²⁺/ZSM-5 may affect the recycle of active sites.

The direct proton transfer from PhCONH₂ to CH₃CN over [Pd]²⁺ was limited by a large energy barrier, the -OH group on [PdOH]⁺ may be the better proton acceptor as an agent because oxygen in -OH group has the higher affinity than nitrogen in -NH₂ group. As displayed in Fig. 7, the conversion of benzamide to benzonitrile would go through four transition states. As an agent, -OH group would accept one proton to be adsorbed water, and this adsorber water as the proton donor would donate the proton to the -CN group, PhCN and CH₃CONH₂ would form after twice proton transfer and C=O bond rupture/formation. By this means, original C=O bond rupture and new C=O bond formation over

[PdOH]⁺ are not so violent like that process over [Pd]²⁺, this is one reason why the maximum energy span of 29.9 kcal/mol over [PdOH]⁺ is smaller than that of 35.8 kcal/mol over [Pd]²⁺. Moreover, the products of PhCN and CH₃CONH₂ are not so tightly adsorbed on [PdOH]⁺ with adsorption energy of 47.9 kcal/mol, which is more benefit to the desorption of products and the recycle of active sites with less energy compensation than [Pd]²⁺. Moreover, despite the adsorption and desorption steps, the overall reaction process is thermodynamically feasible with exothermic energy of 4.9 kcal/mol. Therefore, the reaction process of benzamide to benzonitrile over [PdOH]⁺ is both thermodynamically and kinetically favorable, and the reaction was preferentially catalyzed by [PdOH]⁺ by comparing to [Pd]²⁺.

Review the complete potential energy surface of [PdOH]⁺/ZSM-5 in Fig. 7, four intrinsic energy barriers are 17.5, 17.0, 0.8 and 21.1 kcal/mol, respectively, and the second proton transfer from water to CH₃CN is the rate-determining step. All these reasonable intrinsic and apparent energy barriers are smaller than these of [Pd]²⁺/ZSM-5, which indicated the accuracy of speculation to the structure of [PdOH]⁺ active center. Moreover, differently from the Lewis acid site of Pd in [Pd]²⁺/ZSM-5, the -OH group and Pd in [PdOH]⁺/ZSM-5 act as Brønsted base and Lewis acid, respectively. The synergistic effects of -OH group and Pd in [PdOH]⁺/ZSM-5 promote the conversion of benzamide to benzonitrile.

Based on the [PdOH]⁺ active center with the high catalytic activity to transform benzamide to benzonitrile, the difference in catalytic performance of Pd/Silicalite-1-H and Pd/ZSM-5-H must be explain urgently. In the reaction over [PdOH]⁺/ZSM-5, it's notified that the oxygen in [Pd-OH]⁺ plays a crucial role, and the proton trapping ability of oxygen in [Pd-OH]⁺ directly decided whether the catalytic reaction

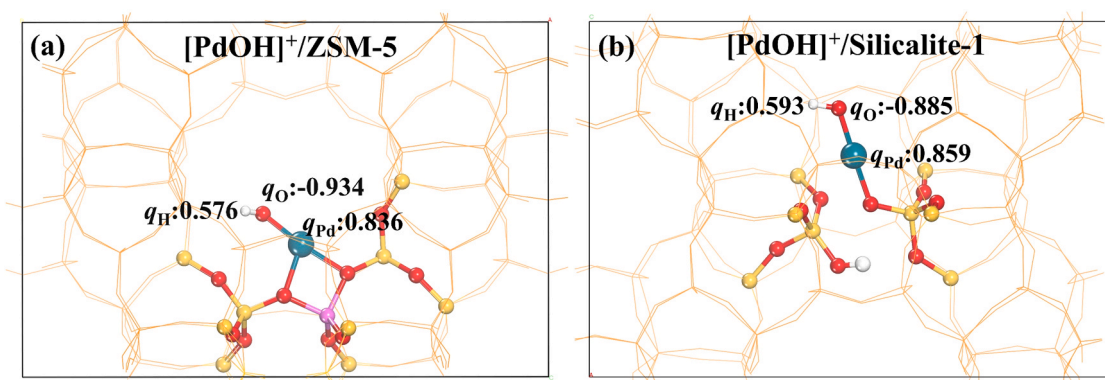


Fig. 8. The Bader atomic charges of [PdOH]⁺ grafted on ZSM-5 and Silicalite-1.

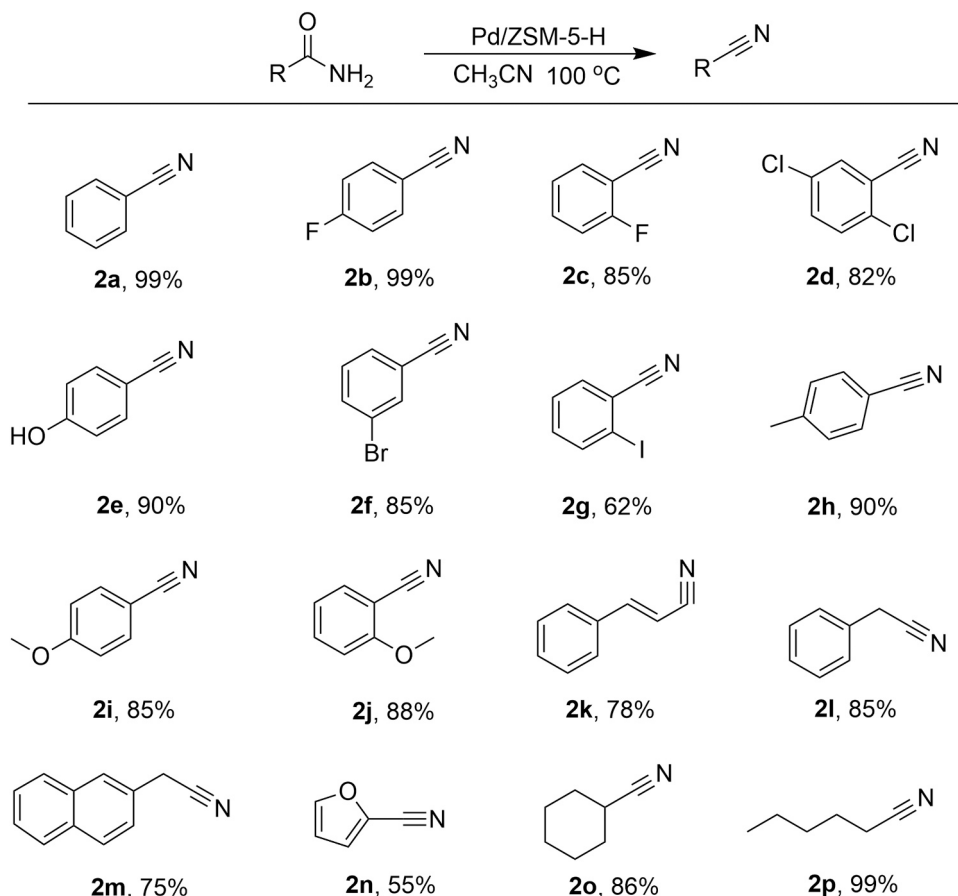


Fig. 9. The reductive of primary amides to nitriles on Pd/ZSM-5-H catalyst. Reaction conditions: Substrate (0.2 mmol), Solvent (2 mL), catalyst (20 mg). Reaction time is 4–6 h. The data was obtained by GC 7890B analysis.

efficiently occurs. The negative charge of oxygen can be used to evaluate its proton trapping ability, the larger negative charge, and the higher catalyzed activity. In this context, the Bader charges of $[\text{Pd}-\text{OH}]^+$ in Pd/Silicalite-1-H and Pd/ZSM-5-H were calculated as shown in Fig. 8, note that the q_{Pd} and q_{H} in Pd-OH on Pd/ZSM-5-H and Pd/Silicalite-1-H is almost the same. But the q_{O} in Pd-OH on Pd/ZSM-5-H catalyst is obviously more negative than that in Pd/Silicalite-1-H, which indicates the higher ability of Pd/ZSM-5-H to capture proton than that in Pd/Silicalite-1-H. Therefore, the $[\text{Pd}-\text{OH}]^+$ on the Pd/ZSM-5-H has the higher catalytic activity than Pd/Silicalite-1-H exactly as experimentally observation in Table 2. This is because the interaction of $[\text{Pd}(\text{II})]$ species with negative charge framework through Brønsted acidic sites on the Pd/ZSM-5-H is stronger than silanol on the Pd/Silicalite-1-H. In this case, the negative charge framework has electron donor characteristics, which should modify the Bader charges of $[\text{Pd}-\text{OH}]^+$ in Pd/ZSM-5-H catalyst and result in more negative charge of the O in $[\text{Pd}-\text{OH}]^+$ structure.

It has been reported that very small metal clusters should have flexible geometry, and easily be modified by zeolite framework, which can influence the adsorption-desorption of the reactant and product [37]. On the other hand, the strong interaction of the small metal clusters with zeolite framework can lead to the change in electronic density and distribution of the metal clusters [38–42]. In our case, most of the $[\text{Pd}-\text{OH}]^+$ clusters even less than 1 nm are embedded in the micropore mouths that open on the mesoporous surface of the ZSM-5-H zeolite. Thus, the negative charge framework of ZSM-5-H can act as a rigid electron ligand for the $[\text{Pd}-\text{OH}]^+$ active center. Meanwhile, the coordination of reactant molecules with Pd-OH active center presents homogeneous catalysis characteristics, which can be called “pseudo-homogeneous catalysis” mode.

It is worth pointing out that the mesopores in the Pd/ZSM-5-H catalyst also play an important role in this transformation. Although the acidities in micropore and mesopore of ZSM-5-H are indistinguishable as displayed in Fig. 2c Pd assembled on ZSM-5 without mesopores (Pd/ZSM-5) shows very low benzamide conversion (16%, entry 14 in Table 2). This could be because the reaction only occurs on the outer surface of the Pd/ZSM-5 catalyst. Because the coordination structure of the benzamide molecule requires a relatively large space, the small size micropore channels (0.53×0.55 nm) in the ZSM-5 crystals cannot satisfy this requirement. In contrast, ZSM-5-H has abundant mesoporosity with mesopore volume of $0.37 \text{ cm}^3 \text{ g}^{-1}$, and the mesopore size about 11 nm is large enough for the requirement of the substrate coordination space. After loading of Pd[II], most Pd species in the form of palladium hydroxides can be highly dispersed into the mesoporous channels of the Pd/ZSM-5-H catalyst, which provided large enough coordination space for the substrate molecules. In this case, the substrate can be dominantly activated in the mesopores of the Pd/ZSM-5-H catalyst.

3.3. Good substrate scope on Pd/ZSM-5-H catalyst

The catalytic performance of the Pd/ZSM-5-H catalyst was further examined by employing various aryl(primary) amides with electron-withdrawing groups (chlorine, bromine, fluorine, iodine and hydroxyl) and electron-donating groups (methoxyl, methyl) at the *para*-, *meta*- or *ortho*-position of the aromatic ring, (Fig. 9) affording the desired products in good yields (2b–2j). Likewise, the unsaturated cinnamamide was also converted smoothly to the nitrile (2k) in 78% yield. In addition, aliphatic linear phenylacetamide was dehydrated to produce the corresponding nitrile (2l) in 85% yield. Interestingly, although 2-

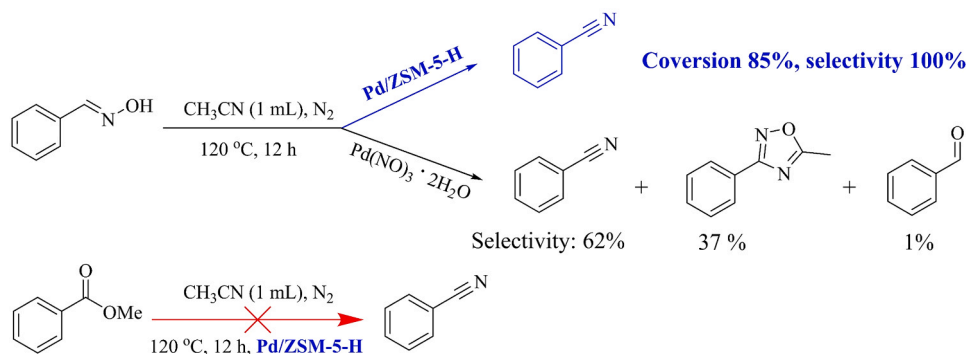


Fig. 10. Catalytic dehydration of benzaldoxime to nitriles on Pd/ZSM-5-H and Pd(NO₃)₂·2H₂O catalysts, and catalytic test of benzoic acid benzyl ester to benzonitrile on Pd/ZSM-5-H.

naphthamide with a large molecular dimension has large spatial steric resistance, it was also successfully applied to this transformation in gratifying yields (**2m**). Heterocyclic amide of 2-furamide was also converted to 2-cyanofuran (**2n**) in moderate yield. It is interesting that the cyclohexanamide and aliphatic caproamide were also converted to corresponding nitrile products (**2o** and **2p**) in high yields. These results indicate that the Pd/ZSM-5-H catalyst has good substrate tolerance. Moreover, Pd/ZSM-5-H has the higher catalytic performance than the other reported heterogenous catalysts (K₂O/SiO₂, vanadium oxide, and TBA₄[α-H₄SiW₁₁O₃₉]) [25–27] according to the higher yield, lower reaction temperature, and shorter reaction time as compared in Table S1. Therefore, Pd/ZSM-5-H is an ideal heterogenous catalysts to convert primary amides to nitriles without any additives.

To the advantage of porous Pd/ZSM-5-H, Pd/ZSM-5-H catalyst can be expanded to the dehydration of benzaldoxime to benzonitrile at the reaction temperature of 120 °C under nitrogen atmosphere in high activity (CONV. 85%) and product selectivity (Select. 100%). In contrast, side reactions would occur and the product selectivity is low by using palladium nitrate catalyst (62%) with the by-product formation of 5-methyl-3-phenyl-1,2,4-oxadiazole (37%) in large molecular size (Fig. 10). Furthermore, Pd/ZSM-5-H has been confirmed the catalytic specificity to amides, carboxylic ester was prevented to convert into nitriles because the -OH or -OR groups in carboxylic ester or carboxylic acid have the poorer coordinated ability with Pd than -NH₂ or -NHR groups in amides, and the -OH or -OR groups would be hard to approach the OH group in [PdOH]⁺, not like amide as displayed in Fig. 7a. Therefore, Pd/ZSM-5-H not only provide highly active Pd(II) site, but also give rise to favorable shape selectivity by the mesopores and micropores, as well as the catalytic specificity to amides.

4. Conclusion

In summary, acidic hierarchical porous ZSM-5-H zeolite assembled palladium catalyst (Pd/ZSM-5-H) was prepared and successfully applied for primary amides to nitriles with high activity and product selectivity in the absence of any additives. The primary amides can be converted to the target products in an equal molecular way, and no side reactions occur over Pd/ZSM-5-H catalyst. The acidic sites on the Pd/ZSM-5-H catalyst are favorable for the adsorption of benzamide molecules, which are also beneficial to coordination-activation of benzamide molecules. The benzamide and acetonitrile molecules can be activated by co-coordination with [Pd-OH]⁺ active sites on Pd/ZSM-5-H. Subsequently, the activated intermediate complex underwent two proton transfer steps to form the benzonitrile. It is notable that the oxygen with more negative charge in [Pd-OH]²⁺ exhibits higher ability to capture proton and favor the proton transfer. Additionally, the mesopores in the Pd/ZSM-5-H is necessary for providing coordination space of reactant molecules with active sites. Herein, the reported reaction pathways and electronic properties give some insightful molecular understandings to

the mechanism of primary amides to nitriles over Pd catalysts, and Pd/ZSM-5-H was found to be an ideal catalyst in the green synthesis route.

CRediT authorship contribution statement

Zhongmiao Chen: Conceptualization, Methodology, Writing – original draft. **Wei Chen:** Methodology, Experimental investigation, Data curation, Writing. **Lei Zhang, Wenqian Fu and Guoren Cai:** Experimental investigation, Data curation. **Anmin Zheng:** Methodology, Conceptualization. **Wei Chen and Tiandi Tang:** Conceptualization, Writing, Supervision.

Declaration of Competing Interest

The authors declare that they have no known competing financial interests or personal relationships that could have appeared to influence the work reported in this paper.

Acknowledgement

This work was supported by the National Natural Science Foundation of China (21776022, 21972011, U1662139 and 22002174).

Appendix A. Supporting information

Supplementary data associated with this article can be found in the online version at doi:10.1016/j.apcatb.2021.120835.

References

- [1] A. Chanda, V.V. Fokin, Organic synthesis “on water”, Chem. Rev. 109 (2009) 725–748.
- [2] M.A. Brimble, Organic synthesis: where to from now? A personal perspective from down under, Org. Lett. 21 (2019) 5773–5774.
- [3] R. Carlson, J.E. Carlson, Design and Optimization in Organic Synthesis: Second Revised and Enlarged Edition, Elsevier Science, 2005.
- [4] R.J.H. Gregory, Cyanohydrins in nature and the laboratory: biology, preparations, and synthetic applications, Chem. Rev. 99 (1999) 3649–3682.
- [5] L.H. Wang Jiang, Application of nitrile in drug design, Chin. J. Org. Chem. 32 (2012) 1643–1652.
- [6] Chapter 10 - Style and usage for organic chemistry, in: H. Rabinowitz, S. Vogel (Eds.), The Manual of Scientific Style, Academic Press, San Diego, 2009, pp. 399–425.
- [7] Z.Y. Cheng, Y.Y. Xia, Z.M. Zhou, Recent advances and promises in nitrile hydratase: from mechanism to industrial applications, Front. Bioeng. Biotechnol. 8 (2020).
- [8] J.E. Callen, C.A. Dornfeld, G.H. Coleman, 9-Cyanophenanthrene: 9-phenanthrenecarbonitrile, Org. Synth. 28 (2003), 34–34.
- [9] G.Y. Popova, T.V. Andrushkevich, Y.A. Chesalov, L.M. Plyasova, L.S. Dovlitova, E. V. Ischenko, G.I. Aleshina, M.I. Khranov, Formation of active phases in MoVTeNb oxide catalysts for ammoxidation of propane, Catal. Today 144 (2009) 312–317.
- [10] M. Ganesan, P. Nagaraaj, Recent developments in dehydration of primary amides to nitriles, Org. Chem. Front. 7 (2020) 3792–3814.
- [11] Y.J. Xia, D.D. He, W.Q. Wu, Recent advances for hydration reaction of nitriles in different catalytic systems, Chin. J. Org. Chem. 41 (2021) 969–982.

- [12] M.H. Al-Huniti, M.P. Croatt, Metal-catalyzed dehydration of primary amides to nitriles, *Asian J. Org. Chem.* 8 (2019) 1791–1799.
- [13] S.A. Shipilovskikh, V.Y. Vaganov, E.I. Denisova, A.E. Rubtsov, A.V. Malkov, Dehydration of amides to nitriles under conditions of a catalytic Appel reaction, *Org. Lett.* 20 (2018) 728–731.
- [14] S.I. Maffioli, E. Marzorati, A. Marazzi, Mild and reversible dehydration of primary amides with PdCl_2 in aqueous acetonitrile, *Org. Lett.* 7 (2005) 5237–5239.
- [15] M.H. Al-Huniti, J. Rivera-Chávez, K.L. Colón, J.L. Stanley, J.E. Burdette, C. J. Pearce, N.H. Oberlies, M.P. Croatt, Development and utilization of a palladium-catalyzed dehydration of primary amides to form nitriles, *Org. Lett.* 20 (2018) 6046–6050.
- [16] S. Shi, M. Szostak, Decarbonylative cyanation of amides by palladium catalysis, *Org. Lett.* 19 (2017) 3095–3098.
- [17] H. Okabe, A. Naraoka, T. Isogawa, S. Oishi, H. Naka, Acceptor-controlled transfer dehydration of amides to nitriles, *Org. Lett.* 21 (2019) 4767–4770.
- [18] W.D. Zhang, C.W. Haskins, Y. Yang, M.J. Dai, Synthesis of nitriles via palladium-catalyzed water shuffling from amides to acetonitrile, *Org. Biomol. Chem.* 12 (2014) 9109–9112.
- [19] S.T. Ding, N. Jiao, Direct transformation of N,N-dimethylformamide to -CN: Pd-catalyzed cyanation of heteroarenes via C-H functionalization, *J. Am. Chem. Soc.* 133 (2011) 12374–12377.
- [20] S.I. Maffioli, E. Marzorati, A. Marazzi, Mild and reversible dehydration of primary amides with PdCl_2 in aqueous acetonitrile, *Org. Lett.* 7 (2005) 5237–5239.
- [21] L. Liu, A. Corma, Isolated metal atoms and clusters for alkane activation: translating knowledge from enzymatic and homogeneous to heterogeneous systems, *Chem* 7 (2021) 2347–2384.
- [22] X.J. Cui, W. Li, P. Ryabchuk, K. Junge, M. Beller, Bridging homogeneous and heterogeneous catalysis by heterogeneous single-metal-site catalysts, *Nat. Catal.* 1 (2018) 385–397.
- [23] D. Astruc, F. Lu, J.R. Aranzas, Nanoparticles as recyclable catalysts: the frontier between homogeneous and heterogeneous catalysis, *Angew. Chem. Int. Ed.* 44 (2005) 7852–7872.
- [24] J. Blum, A. Fisher, E. Greener, The catalytic decomposition of secondary carboxamides by transition-metal complexes, *Tetrahedron* 29 (1973) 1073–1081.
- [25] Y.M. Li, Y.J. Zhao, S.P. Wang, X.B. Ma, Silica supported potassium oxide catalyst for dehydration of 2-picolinamide to form 2-cyanopyridine, *Chin. Chem. Lett.* 30 (2019) 494–498.
- [26] S. Sueoka, T. Mitsudome, T. Mizugaki, K. Jitsukawa, K. Kaneda, Supported monomeric vanadium catalyst for dehydration of amides to form nitriles, *Chem. Commun.* 46 (2010) 8243–8245.
- [27] S. Itagaki, K. Kamata, K. Yamaguchi, N. Mizuno, A. Monovacant, Lacunary silicotungstate as an efficient heterogeneous catalyst for dehydration of primary amides to nitriles, *ChemCatChem* 5 (2013) 1725–1728.
- [28] J.A. Campbell, G. McDougald, H. McNab, L.V.C. Rees, R.G. Tyas, Laboratory-scale synthesis of Nitriles by catalysed dehydration of Amides and Oximes under flash vacuum pyrolysis (FVP) conditions, *Synthesis* 20 (2007) 3179–3184.
- [29] P. Gelin, M. Primet, Complete oxidation of methane at low temperature over noble metal based catalysts: a review, *Appl. Catal. B Environ.* 39 (2002) 1–37.
- [30] A.W. Petrov, D. Ferri, F. Krumeich, M. Nachtegaal, J.A. van Bokhoven, O. Krocher, Stable complete methane oxidation over palladium based zeolite catalysts, *Nat. Commun.* 9 (2018) 2545.
- [31] A.W. Petrov, D. Ferri, O. Krocher, J.A. van Bokhoven, Design of stable palladium-based zeolite catalysts for complete methane oxidation by postsynthesis zeolite modification, *ACS Catal.* 9 (2019) 2303–2312.
- [32] I. Friberg, N. Sadokhina, L. Olsson, The effect of Si/Al ratio of zeolite supported Pd for complete CH₄ oxidation in the presence of water vapor and SO₂, *Appl. Catal. B Environ.* 250 (2019) 117–131.
- [33] C.T. Wang, L. Wang, J. Zhang, H. Wang, J.P. Lewis, F.S. Xiao, Product selectivity controlled by zeolite crystals in biomass hydrogenation over a palladium catalyst, *J. Am. Chem. Soc.* 138 (2016), 13756–13756.
- [34] C.T. Wang, Z.Q. Liu, L. Wang, X. Dong, J. Zhang, G.X. Wang, S.C. Han, X.J. Meng, A.M. Zheng, F.S. Xiao, Importance of zeolite wettability for selective hydrogenation of furfural over Pd@Zeolite catalysts, *ACS Catal.* 8 (2018) 474–481.
- [35] W.Q. Fu, Y. Feng, Z.X. Fang, Q. Chen, T. Tang, Q.Y. Yu, T.D. Tang, Zeolite Y nanosheet assembled palladium catalysts with high catalytic activity and selectivity in the vinylation of thiophenes, *Chem. Commun.* 52 (2016) 3115–3118.
- [36] S. Zhao, S. He, K.D. Kim, L. Wang, R. Ryoo, Z. Wang, J. Huang, Influence of hierarchical ZSM-5 catalysts with various acidity on the dehydration of glycerol to acrolein, *Magn. Reson. Lett.* 1 (2021) 71–80.
- [37] Y. Zheng, L. Kovarik, M.H. Engelhard, Y.L. Wang, Y. Wang, F. Gao, J. Szanyi, Low-temperature Pd/zeolite passive NO_x adsorbers: structure, performance, and adsorption chemistry, *J. Phys. Chem. C* 121 (2017) 15793–15803.
- [38] E.M. Fernandez, J.M. Soler, I.L. Garzon, L.C. Balbas, Trends in the structure and bonding of noble metal clusters, *Phys. Rev. B* 70 (2004), 165403.
- [39] G.N. Vayssilov, Y. Lykhach, A. Migani, T. Staudt, G.P. Petrova, N. Tsud, T. Skala, A. Bruix, F. Illas, K.C. Prince, V. Matolin, K.M. Neyman, J. Libuda, Support nanostructure boosts oxygen transfer to catalytically active platinum nanoparticles, *Nat. Mater.* 10 (2011) 310–315.
- [40] M. Kitano, Y. Inoue, Y. Yamazaki, F. Hayashi, S. Kanbara, S. Matsuishi, T. Yokoyama, S.W. Kim, M. Hara, H. Hosono, Ammonia synthesis using a stable electride as an electron donor and reversible hydrogen store, *Nat. Chem.* 4 (2012) 934–940.
- [41] S. Kanbara, M. Kitano, Y. Inoue, T. Yokoyama, M. Hara, H. Hosono, Mechanism switching of ammonia synthesis over Ru-loaded electride catalyst at metal-insulator transition, *J. Am. Chem. Soc.* 137 (2015) 14517–14524.
- [42] Z. Li, S.F. Ji, Y.W. Liu, X. Cao, S.B. Tian, Y.J. Chen, Z.G. Niu, Y.D. Li, Well-defined materials for heterogeneous catalysis: from nanoparticles to isolated single-atom sites, *Chem. Rev.* 120 (2020) 623–682.